



# Investigation into patterning of a stack-type Ru electrode capacitor

Hyoun Woo Kim<sup>a,\*</sup>, Chang-Jin Kang<sup>b</sup>

<sup>a</sup>*School of Materials Science and Engineering, Inha University, Incheon 402-751, South Korea*

<sup>b</sup>*Semiconductor Research & Development Center, Samsung Electronics, Kyungki-Do 449-900, South Korea*

Received 26 October 2002; received in revised form 27 February 2003; accepted 7 April 2003

---

## Abstract

We have investigated the characteristics of etching processes involved in the fabrication of the stack-type DRAM capacitor. The 4000-Å high Ru electrode and the SiO<sub>2</sub> hard mask with a critical dimension of 0.15 μm were employed. The Ru etch rate and the Ru to SiO<sub>2</sub> mask etch selectivity increased by increasing pressure, total gas flow rate, and by addition of Cl<sub>2</sub> gas. We have removed the SiO<sub>2</sub> mask residues using Ar/CHF<sub>3</sub> plasmas, revealing that high RF power helps to remove the residue efficiently.

© 2003 Elsevier B.V. All rights reserved.

*Keywords:* Ru; Etching; SiO<sub>2</sub> mask; Scanning electron microscopy

---

## 1. Introduction

As dimensions of devices are getting smaller and smaller, high dielectric materials, such as barium strontium titanate (BST), tantalum pentoxide (Ta<sub>2</sub>O<sub>5</sub>), need to be used for the fabrication of dynamic random access memory (DRAM) capacitors [1–4].

Capacitors based on dielectric materials need to employ electrode materials, which should remain stable during the fabrication process. For this reason, noble metals and refractory oxides such as platinum (Pt), ruthenium (Ru), and ruthenium oxide (RuO<sub>2</sub>) have been intensively considered. Although Pt has been usually investigated as an electrode material, Pt has an etching problem. Several research groups have reported that obtaining the sufficient etching slope of Pt electrode is very difficult due to the sputtering-nature of the Pt etching process [5–9].

On the other hand, Ru or RuO<sub>2</sub> is expected to be patterned by dry etching because the volatile etch

---

\*Corresponding author. Tel.: +82-32-860-7544; fax: +82-32-862-5546.

E-mail address: [hwkim@inha.ac.kr](mailto:hwkim@inha.ac.kr) (H.W. Kim).

product can be produced [10–14]. In patterning the Ru electrode, the conventional photoresist mask cannot be used because the  $O_2$ -based plasma needs to be used for Ru etching. Even though there are some reports on the basic characteristics of Ru etching [12,13], there is rare report on the fabrication of Ru electrode in real device pattern.

In this work, we report on the Ru etching process related to the fabrication of stack-type Ru electrode. We report the etching characteristics of Ru using  $O_2/Cl_2$  helicon plasmas. We investigate the variation of Ru etch rate and the Ru etching slope with varying process conditions including pressure, total gas flow rate, and  $Cl_2/(O_2 + Cl_2)$  gas flow ratio. We also investigate the removal process of the remaining  $SiO_2$  mask after Ru etching, by using wet etching or dry etching technique.

## 2. Experiments

A storage node pattern with a critical dimension (CD) of 0.15  $\mu m$  was used in our experiments. Top view of the storage node pattern indicates that the storage node is an oval type and space CDs along the short axis and the long axis are 150 and 250 nm, respectively. The sample structure was Si substrate/ $SiO_2$  layer/ $TiO_2$  600 Å/Ru 4000 Å/ $SiO_2$  mask 2000 Å. For some device wafers, the  $TiO_2$  layer was removed and the Ru electrode layer was directly deposited on the  $SiO_2$  layer. The  $SiO_2$  mask, instead of photoresist mask, was used for patterning Ru, because oxygen gas was the main etchant in our experiments. In another set of experiments dealing with the removal of  $SiO_2$  mask layer, the gate pattern was used.

An e-MxP+ chamber, commercially available from Applied Materials, has been used for  $SiO_2$  mask etching. The  $SiO_2$  mask was patterned by  $CHF_3/CF_4/N_2/Ar$  gas with an RF power of 1100 W and a magnetic field of 30 gauss. The relatively high RF power was employed to obtain the vertical profile of the  $SiO_2$  mask and the high gas flow ratio of  $CHF_3/CF_4$  is employed in order to minimize the bowing and undercut of patterned  $SiO_2$  mask.

Schematic diagram of a helicon plasma reactor used for Ru electrode etching is shown in our previous work [13]. During etching, the source power was set to 2000 W, the bias power was set to 200 W, the pressure ranged from 10 to 30 mTorr and the total gas flow rate ranged from 50 to 300 sccm. The cathode temperature was set to 45 °C and the helium pressure for cathode cooling was set to 15 Torr.

As Ru cannot be etched by halogen gases due to high boiling point of their etch products, we used  $O_2$  gas as a main etchant, expecting that the volatile  $RuO_4$  is produced [11,12]. The  $Cl_2$  gas was added to enhance the etch rate.

A scanning electron microscope (SEM) was used to observe the top and vertical view of the Ru electrode pattern after etching process. In order to prepare a sample for the vertical SEM observation, a wafer was cut along the short axis of storage node patterns.

## 3. Results and discussion

### 3.1. Patterning of Ru electrode layer

To investigate the etching characteristics of Ru electrode using  $O_2/Cl_2$  helicon plasma,  $Cl_2/(O_2 + Cl_2)$  gas flow ratio, total gas flow rate, and pressure were varied. Fig. 1a,b shows the change of Ru

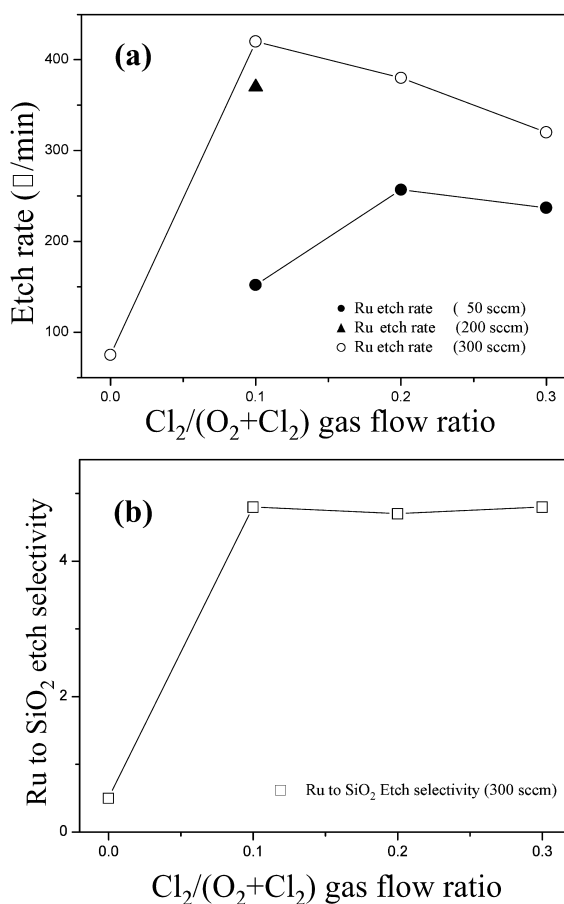


Fig. 1. (a) Change of Ru etch rate by varying  $\text{Cl}_2/(\text{O}_2 + \text{Cl}_2)$  gas flow ratio, Pressure ranges from 50 to 300 sccm. (b) Change of Ru to  $\text{SiO}_2$  etch selectivity by varying  $\text{Cl}_2/(\text{O}_2 + \text{Cl}_2)$  gas flow ratio at a pressure of 300 sccm.

etch rate and the change of Ru to  $\text{SiO}_2$  etch selectivity, respectively, by varying  $\text{Cl}_2/(\text{O}_2 + \text{Cl}_2)$  gas flow ratio in the range of 0.1 to 0.3, revealing that the Ru etch rate increases from 75 to 420  $\text{\AA}/\text{min}$  by increasing the  $\text{Cl}_2/(\text{O}_2 + \text{Cl}_2)$  gas flow ratio from 0 to 0.1 when etched with a total gas flow rate of 300 sccm. Etching with  $\text{O}_2$  plasma results in the Ru to  $\text{SiO}_2$  etch selectivity of about 0.5 and etching with  $\text{Cl}_2/\text{O}_2$  plasma results in the Ru to  $\text{SiO}_2$  etch selectivity of more than 4, when etched with a total gas flow rate of 300 sccm. Since the Ru etch rate significantly increases by adding  $\text{Cl}_2$  gas, we surmise that  $\text{Cl}_2$  plays a catalytic role in generating the volatile  $\text{RuO}_2$  during the etching process. When etched with a total gas flow rate of 50 sccm, the optimal  $\text{Cl}_2/(\text{O}_2 + \text{Cl}_2)$  gas flow ratio increases compared to when etched at 300 sccm.

Fig. 1a also reveals that the Ru etch rate increases by increasing the total gas flow rate ranging from 50 to 300 sccm. When etched with a  $\text{Cl}_2/(\text{O}_2 + \text{Cl}_2)$  gas flow ratio of 0.1, the Ru etch rates are 152, 370, and 420  $\text{\AA}/\text{min}$ , respectively, at the pressure of 50, 200, and 300 mTorr. Our experiments reveals that the Ru etch rate and Ru etching slope increase by increasing total gas flow rate [13]. We surmise that the amount of radical flux per unit time may increase and thus the Ru etching reaction may be enhanced with increasing the total gas flow rate.

In order to investigate the role of Ar in Ru etching, we have added Ar gas to  $O_2/Cl_2$  plasma. We have added 0, 5, and 10 sccm of Ar gas for comparison study, with the total gas flow rate of 50 sccm. In order to exclude the effect of  $O_2$  or  $Cl_2$ , the  $Cl_2/(O_2 + Cl_2)$  gas flow ratio is fixed to 0.2 in this experiment. Fig. 2 shows that when  $Ar/(O_2 + Cl_2 + Ar)$  gas flow ratios are 0, 0.1, and 0.2, respectively, Ru etch rates are 280, 312, and 337 Å/min. We reveal that the Ru etch rate slightly increases by increasing the  $Ar/(O_2 + Cl_2 + Ar)$  gas flow ratio.

In order to investigate the effect of pressure, we have performed the Ru electrode etching at pressures ranging from 10 to 30 mTorr. The total gas flow rate, the  $Cl_2/(Cl_2 + O_2)$  gas flow rate, and bias power are set to 300 sccm, 0.2, and 250 W, respectively. Ru etch rates are 300, 500, and 560 Å/min. Ru to  $SiO_2$  etch selectivities are 1.1, 3.4, and 5.5 at a pressure of 10, 20, and 30 mTorr, respectively. Ru etching sidewall slopes are  $45^\circ$ ,  $78^\circ$ , and  $87^\circ$ , respectively, at a pressure of 10, 20, and 30 mTorr.

Fig. 3 shows SEM images of Ru etching profile at a pressure of (a) 20 mTorr and (b) 30 mTorr. Samples are processed with 20% of an overetch after end point detection (EPD). It is noteworthy that the post-etch Ru surface etched at 20 mTorr is relatively rough compared to the surface etched at 30 mTorr. Furthermore, the amount of remaining  $SiO_2$  mask after the etching process is smaller in case of 20 mTorr. We suppose that the Ru etching using  $SiO_2$  mask at a pressure of 30 mTorr is more efficient than that at 20 mTorr from the above result. Further systematic studies are necessary to reveal the detailed effect of pressure on Ru etching process.

### 3.2. Removal of mask layer

When the etching process has a high etch selectivity of Ru to  $SiO_2$ ,  $SiO_2$  mask residues are remaining on top of the Ru electrode as shown in Fig. 3b, even after completing the etching process. We have applied the wet etching technique using a mixture of deionized water and hydrofluoric acid (HF). The process is effective in removing the  $SiO_2$  mask residues but the surface of the Ru electrode

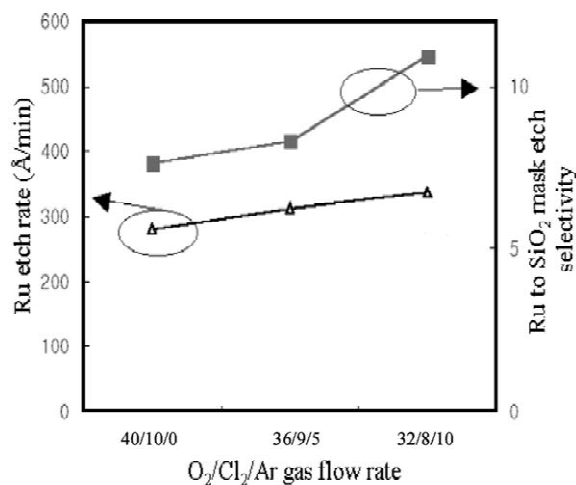
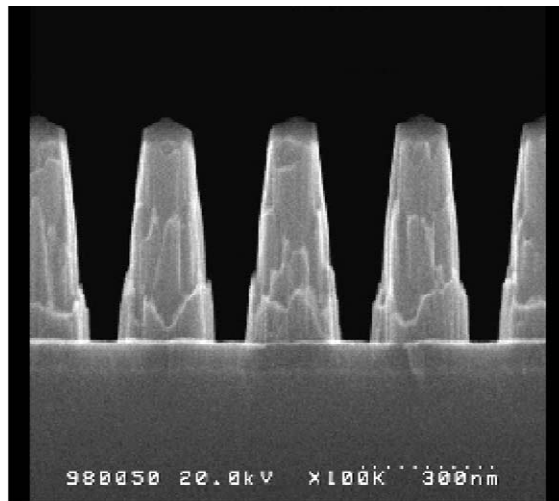
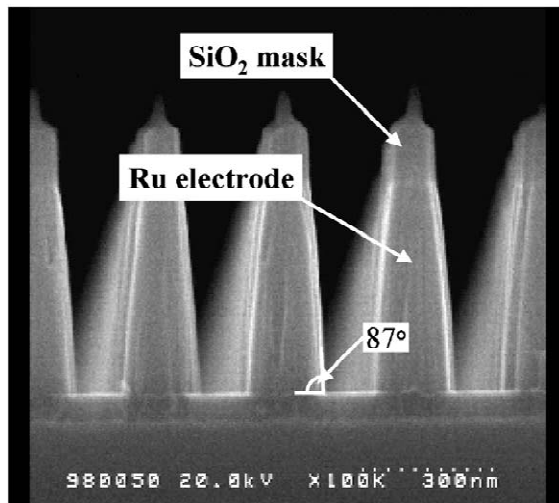


Fig. 2. Change of Ru etch rate, Ru to  $SiO_2$  etch selectivity depending on the  $O_2/Cl_2/Ar$  gas flow ratio.



(a)



(b)

Fig. 3. SEM images of Ru etching profile etched at (a) 20 mTorr and (b) 30 mTorr.

becomes very rough due to the reaction of HF with the Ru atoms. Fig. 4 shows the SEM images of Ru etching profile with the bottom layer of TiO<sub>2</sub>. When the bottom layer is SiO<sub>2</sub>, the SiO<sub>2</sub> layer is attacked by the HF aqueous solution and the storage node is collapsed (not shown here).

Accordingly, we have performed an experiment to remove the SiO<sub>2</sub> mask residue by plasma etching using Ar/CHF<sub>3</sub> system. We have used a gate electrode pattern in which Ru was partially

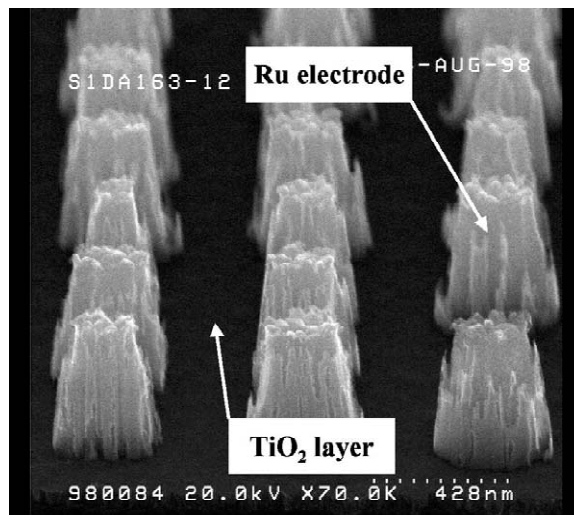


Fig. 4. SEM images of Ru etching profile with the bottom layer of  $\text{TiO}_2$ .

etched. As shown in Fig. 5a, the mask residues of the irregular shapes are remained even by 100% overetch. We surmise that the mask  $\text{SiO}_2$  layer reacts with the Ru surface by the supplied thermal energy during etching process and thus the adhesive  $\text{RuO}_x$ -type compounds are generated between the mask  $\text{SiO}_2$  and Ru surface.

We have performed an experiment to remove the  $\text{SiO}_2$  mask residue by elevating the RF power from 250 to 600 W. By applying the high-RF power etching process, the  $\text{SiO}_2$  mask sidewall residues on top of Ru electrode are removed completely without the excessive etching. Fig. 5b,c shows the top view and the cross-sectional view of the Ru etching profile with the  $\text{SiO}_2$  mask removed by high power etching process. However, it is notable that the Ru etching slope is lowered during the mask removal etching, probably resulting from the resputtering of Ru atoms.

When we use the  $\text{SiO}_2$  as a bottom layer instead of  $\text{TiO}_2$  layer, considerable amount of the bottom layer is eroded during the mask removal process even by applying the dry-etching method. To overcome this problem, we investigated replacement of the  $\text{SiO}_2$  mask layer with the  $\text{SiON}$  layer. In this case, we performed the Ru electrode etching using the  $\text{SiON}$  mask and then removing the remaining  $\text{SiON}$  mask by the optimal etching process which has a sufficient  $\text{SiON}$  to  $\text{SiO}_2$  etch selectivity. Subsequently, we remove the remained mask residue by wet etching method using the phosphoric acid which is expected to have a sufficient  $\text{SiON}$  to  $\text{SiO}_2$  etch selectivity.

#### 4. Conclusion

We have investigated the characteristics of etching processes involved in the fabrication of DRAM capacitors using a stack-type Ru electrode. The variation of Ru etch rate and Ru etching slope by varying process parameters using  $\text{O}_2/\text{Cl}_2$  helicon plasmas, such as  $\text{Cl}_2/(\text{O}_2 + \text{Cl}_2)$  gas flow ratio, total flow rate, and pressure has been investigated. Ru etch rate and Ru to  $\text{SiO}_2$  mask etch selectivity increase by increasing the total gas flow rate, and addition of  $\text{Cl}_2$  gas, implying the importance of

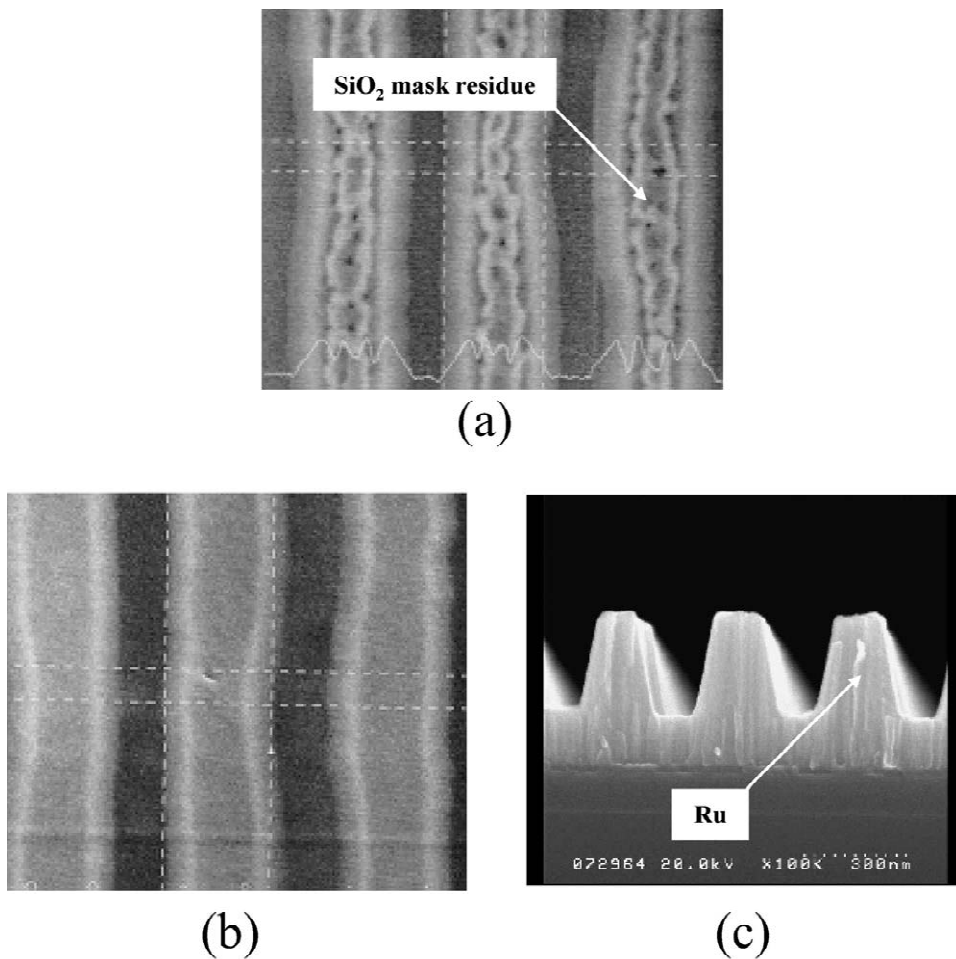


Fig. 5. SEM images of Ru gate patterns showing the removal of SiO<sub>2</sub> mask. (a) Top view of the patterns etched with a low (250 W) RF power. (b) Top view of the patterns etched with a high (600 W) RF power. (c) Cross-sectional view of the patterns etched with a high (600 W) RF power.

chemical reaction for the efficient Ru etching. It is noteworthy that Ru to SiO<sub>2</sub> etch selectivity and thus Ru etching sidewall slope increase by increasing the pressure. In order to remove the SiO<sub>2</sub> mask residues after the Ru etching, we apply both wet etching and dry etching techniques. In the dry etching technique using Ar/CHF<sub>3</sub> plasmas, we reveal that high RF power helps to remove the SiO<sub>2</sub> mask residues efficiently.

### Acknowledgements

The authors gratefully acknowledge financial support of present work by Semiconductor Research & Development Center of Samsung electronics Co. We especially thank to Dr. Moon Yong Lee and

Dr. Joo Tae Moon for their advice. Also this work was supported by INHA UNIVERSITY Research Grant through the Special Research Program in 2003.

## References

- [1] S. Yamamichi, P.-Y. Lesaicherre, H. Yamaguchi, K. Takemura, S. Sone, H. Yabuta, K. Sato, T. Tamura, K. Nakajima, S. Ohnishi, K. Tokashiki, Y. Hayashi, Y. Kato, Y. Miyasaka, M. Yoshida, H. Ono, IEDM 1995 Tech. Digest (1995) 119.
- [2] A. Yuuki, M. Yamamuka, T. Makita, T. Horikawa, T. Shibano, N. Hirano, H. Maeda, N. Mikami, K. Ono, H. Ogata, H. Abe, IEDM 1995 Tech. Digest (1995) 115.
- [3] B.T. Lee, K.H. Lee, C.S. Hwang, W.D. Kim, H. Horii, H.-W. Kim, H.-J. Cho, C.S. Kang, J.H. Chung, S.I. Lee, M.Y. Lee, IEDM Tech. Digest (1997) 249.
- [4] T. Aoyama, S. Yamazaki, K. Imai, J. Electrochem. Soc. 145 (8) (1998) 2961.
- [5] W.J. Yoo, J.H. Hahm, H.W. Kim, C.O. Jung, Y.B. Koh, M.Y. Lee, Jpn. J. Appl. Phys. 35 (1995) 2501.
- [6] K. Nishikama, Y. Kusumi, T. Oomori, M. Hanazaki, K. Namba, Jpn. J. Appl. Phys. 32 (1993) 6102.
- [7] S. Yokoyama, Y. Ito, K. Ishihara, K. Hamada, S. Ohnishi, J. Kudo, K. Sakiyama, Jpn. J. Appl. Phys. 34 (1995) 767.
- [8] H.W. Kim, B.-S. Ju, C.-J. Kang, J.-T. Moon, Microelectron. Eng. 65 (2003) 185.
- [9] T. Shibano, T. Oomori, J. Vac. Sci. Technol. B 15 (5) (1997) 1747.
- [10] S. Saito, K. Kuramasu, Jpn. J. Appl. Phys. 31 (1) (1992) 135.
- [11] W. Pan, S.B. Desu, J. Vac. Sci. Technol. B 12 (6) (1994) 3208.
- [12] K. Tokashiki, in: Proceedings of SEMI Technology Symposium, 1996, pp. 5–46.
- [13] H.W. Kim, J.-H. Han, B.-S. Ju, C.-J. Kang, J.-T. Moon, Mater. Sci. Eng. B95 (2002) 249.
- [14] E.-J. Lee, J.-W. Kim, W.-J. Lee, Jpn. J. Appl. Phys. 37 (1998) 2634.